Structure of excited states in ^{21}Mg studied in one-neutron knockout

C. Aa. Diget,[1,*] P. Adrich,[1] D. Bazin,[1] M. D. Bowen,[1,2] B. A. Brown,[1,2] C. M. Campbell,[1] J. M. Cook,[1,2] A. Gade,[1,2] T. Glasmacher,[1,2] K. Hosier,[3] S. McDaniel,[1,2] D. McGlinchery,[3] A. Obertelli,[1] L. A. Riley,[3] K. Siwek,[1,2] J. R. Terry,[1,2] J. A. Tostevin,[4] and D. Weisshaar[1]

[1]*National Superconducting Cyclotron Laboratory, Michigan State University, East Lansing, Michigan 48824, USA*

[2]*Department of Physics and Astronomy, Michigan State University, East Lansing, Michigan 48824, USA*

[3]*Department of Physics and Astronomy, Ursinus College, Collegeville, Pennsylvania 19426, USA*

[4]*Department of Physics, Faculty of Engineering and Physical Sciences, University of Surrey, Guildford, Surrey GU2 7XH, United Kingdom*

(Received 21 November 2007; published 11 June 2008; publisher error corrected 13 June 2008)

Bound excited states in the neutron-deficient nucleus ^{21}Mg were probed in the one-neutron knockout reaction ^{9}Be(^{22}Mg, ^{21}Mg+γ)X at 74 MeV/nucleon projectile energy. The low-lying level scheme of ^{21}Mg was investigated for the first time with γ-ray spectroscopy. Contrary to the interpretation of previous particle spectroscopy data, our proposed excitation scheme is in agreement with the mirror nucleus and shell-model calculations in the *p-sd* shell. Spectroscopic factors for the one-neutron removal from ^{22}Mg to ^{21}Mg are extracted and compared to shell-model calculations using the WBP effective interaction.

DOI: 10.1103/PhysRevC.77.064309 PACS number(s): 23.20.Lv, 21.10.Jx, 21.60.Cs, 27.30.+t

I. INTRODUCTION

The identification of excited-state properties of ^{21}Mg is crucial for the description of the ^{20}Na(p, γ)^{21}Mg reaction that is important for hydrogen burning in explosive scenarios such as x-ray bursts [1]. In a recent resonant ^{20}Na+p scattering experiment by Ref. [2], the spins and proton widths of some excited states above the proton threshold of S_p = 3226 keV [3] have been determined, and a good correspondence between shell-model calculations and measurements in the region above 4 MeV has been achieved [2]. Based on this agreement it was recommended to include states predicted by the shell model just above the proton threshold in the ^{20}Na(p, γ)^{21}Mg reaction rate calculations, states for which the experimental evidence is less conclusive; in particular spin assignments are lacking. Also, the spectroscopic factors for the bound states are included in the reaction rate calculations, as the direct capture rates to bound states of ^{21}Mg are scaled by the one-proton spectroscopic factors of the states [1]. These spectroscopic factors must be taken from calculations, of which shell-model calculations in the *p-sd* shell are at present the most reliable. However, below the ^{21}Mg proton-separation energy, inconsistencies between experimental and theoretical level assignments have been reported [2]. These inconsistencies warrant clarification in light of the importance of the shell-model input to the astrophysical reaction-rate calculations.

The structure of ^{21}Mg has previously been probed in the three-neutron-transfer reaction, ^{24}Mg(^{3}He,^{6}He)^{21}Mg [4–7], and several states have been identified. In the most recent experiment, restrictions on spin and parity for some bound and unbound states were deduced from the measured angular distributions in the transfer reaction [4]. The excited-state properties of ^{21}Mg were evaluated by Ref. [8] and are shown in Fig. 1(c) for levels below or near the proton threshold. This level scheme for ^{21}Mg is also compared to the excitation pattern of the mirror nucleus ^{21}F [Fig. 1(a)]. For ^{21}Mg, the spin and parity of the first excited state has been determined unambiguously. For several other states below the proton threshold, however, the identification of spin and parity is not unique and the final assignments are largely based on comparison with the mirror nucleus. This is the case for the states around 1 and 2 MeV, for which the experimental assignments were consistent with the properties of the mirror nucleus but not uniquely determined from the existing data. The experimental spin and parity assignment for the 1649-keV state, however, though not unique, was inconsistent with the well-known properties of the corresponding states in the mirror nucleus.

The measured level scheme of ^{21}Mg may furthermore be compared to shell-model calculations. The *p-sd* shell model is well established in this region of the nuclear chart, and one would expect good agreement between experiment and calculations. Figure 1(b) shows the ^{21}Mg level scheme as calculated in the shell model using the NuShell@MSU code [9] with the WBP effective interaction [10]. The model space of *s-p-sd-pf* is truncated to $0\hbar\omega$(*sd* shell) for positive-parity states and $1\hbar\omega$ for negative-parity states. The wave functions for low-lying negative parity states in ^{21}Mg are dominated by configurations with a single hole in the *p* shell. (The $0\hbar\omega$ obtained with the recent USDA and USDB *sd*-shell interactions [11] are similar to those for WBP that contained the original USD interaction for the *sd*-shell part.) A striking observation is that the experimentally proposed properties [Fig. 1(c)] of the 1649-keV state ($J^\pi = 1/2^-, 3/2^-$) could not be reproduced by the *p-sd* shell-model calculations. In this energy region, only a $9/2^+$, $3/2^+$ energy doublet is predicted by theory, states that have not been identified experimentally in ^{21}Mg, though—as seen in Fig. 1(a)—the doublet is known in the mirror nucleus ^{21}F. This inconsistency between theory and

*diget@nscl.msu.edu

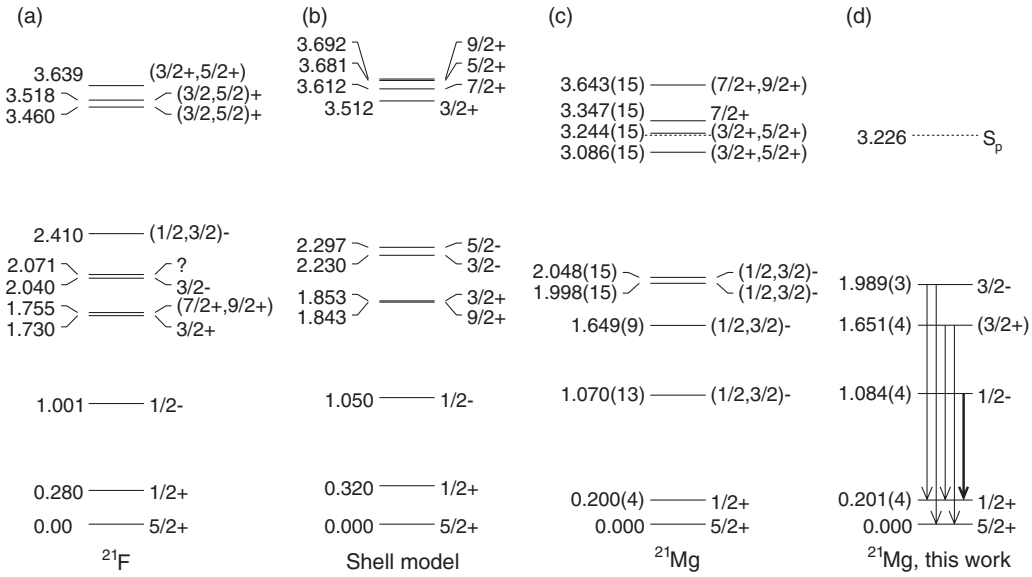

FIG. 1. Experimental level schemes for the mirror nuclei ^{21}F (a) and ^{21}Mg (c) [8], compared to results from a WBP shell-model calculation (b). In (d) we show the ^{21}Mg decay scheme as proposed in the present work. All energies are in MeV, only states below 3.7 MeV are shown.

experiment is important to address to determine the reliability of the shell-model calculations and—if possible—justify their use in the calculation of astrophysical reaction rates in this mass region in general and for the ^{20}Na$(p,\gamma)^{21}$Mg reaction in particular. Another notable feature is a significant energy shift for the $1/2^+$ first excited state in the $A = 21$ mirror nuclei, $E(1/2^+) = 200$ keV in ^{21}Mg, and $E(1/2^+) = 280$ keV in ^{21}F.

In the present article we report on the first study of ^{21}Mg with γ-ray spectroscopy. Excited states in this nucleus were populated in the one-neutron knockout reaction ^{9}Be(^{22}Mg,^{21}Mg$+\gamma$)X at 73.8 MeV/nucleon. Cross sections for the knockout leading to individual final states in ^{21}Mg were measured. From these, spectroscopic factors were extracted with the help of reaction theory formulated in the eikonal and sudden approximations [12,13]. Our new experimental results are compared to shell-model calculations using the WBP effective interaction.

In the following, the experimental method will be introduced (Sec. II), and the results will be discussed (Sec. III) in comparison to shell-model calculations and the mirror nucleus.

II. EXPERIMENTAL METHOD

Direct one-nucleon knockout reactions from intermediate-energy rare-isotope beams have been established as a precision spectroscopic tool to assess the single-particle properties of short-lived, exotic nuclei [14,15]. On surface collision with a light target, typically ^{9}Be, a nucleon is removed and single-hole states are selectively populated in the projectile-like residue. γ-ray spectroscopy is used to identify the final state and to determine the cross section for the population of individual states. The shape of the parallel momentum distribution of the projectile-like knockout residues depends on the orbital angular momentum of the knocked-out nucleon (ℓ value) [14, 16,17].

The reaction ^{9}Be(^{22}Mg,^{21}Mg)X populates one-neutron-hole states in ^{21}Mg relative to the ^{22}Mg ground state. With 10 neutrons in ^{22}Mg, sd-shell single-neutron states relative to ^{20}Mg are populated if one of the two sd-shell valence neutrons is removed, or alternatively, if a neutron is knocked-out from within the $N = 8$ core, negative-parity neutron-hole states are populated in ^{21}Mg.

A. Beam production

The radioactive ^{22}Mg beam was produced at the Coupled-Cyclotron Facility at NSCL [18], on the campus of Michigan State University. This secondary beam was produced by fragmentation of a 150 MeV/nucleon ^{36}Ar primary beam impinging on an 893 mg/cm^2 ^{9}Be target located at the midacceptance target position of the A1900 fragment separator [19]. The fragments were separated in the A1900 separator using a 300-mg/cm^2 achromatic aluminum wedge in conjunction with momentum slits at 0.5% momentum acceptance at the A1900 dispersive image. This yielded a secondary cocktail beam with ^{24}Si, ^{23}Al, ^{22}Mg, ^{21}Na, ^{20}Ne, and ^{19}F components. The individual constituents of the cocktail beam were distinguished on an event-by-event basis from the time-of-flight measured between two plastic scintillators located before the reaction target and separated by about 25 m. This yielded an unambiguous identification of the incoming ^{22}Mg projectiles as described in Ref. [20], where the same experimental setup and cocktail beam was used for the investigation of ^{20}Mg in the two-neutron knockout reaction from ^{22}Mg.

B. Reaction product identification

The secondary beam impinged upon the 188-mg/cm^2 ^{9}Be reaction target placed at the target position of the S800

spectrograph [21]. The spectrograph was operated in focus mode, where the beam is momentum focused onto the reaction target. The beam energy at midtarget for the ^{22}Mg beam was 73.8 MeV/nucleon. With the focal-plane detectors [22] of the spectrograph, the reaction residues were identified and characterized event by event. The energy loss was measured with the ionization chamber of the S800 focal-plane detector system [22]. The residue's time-of-flight through the S800 spectrograph was determined using the S800 focal-plane trigger plastic scintillator in conjunction with a timing scintillator positioned upstream from the reaction target at the object position of the spectrograph. From position measurements performed with the two position-sensitive cathode readout drift chambers (CRDCs) in the S800 focal plane, the residue's flight path through the spectrograph was reconstructed event by event using the optics code COSY [23] in conjunction with the known magnet settings of the spectrograph. With this, the parallel momentum distribution of the knockout residues was reconstructed from the ion's measured position in the S800 focal plane.

The trajectory reconstruction also allowed for the correction of the time-of-flight and of the energy loss so that a very clean particle identification could be obtained. The particle identification for residues produced by incoming ^{22}Mg projectiles is shown in Fig. 2.

C. γ-ray spectroscopy

The secondary target was surrounded by the segmented germanium array SeGA [24]. With SeGA, prompt γ rays were measured in coincidence with the projectile-like residues identified in the S800 spectrograph. The array was equipped with sixteen 32-fold segmented high-purity-germanium detectors. Efficiency and energy calibrations were performed with standard ^{57}Co, ^{152}Eu, and ^{226}Ra sources yielding a relative uncertainty on the absolute scale of the efficiency of 5%.

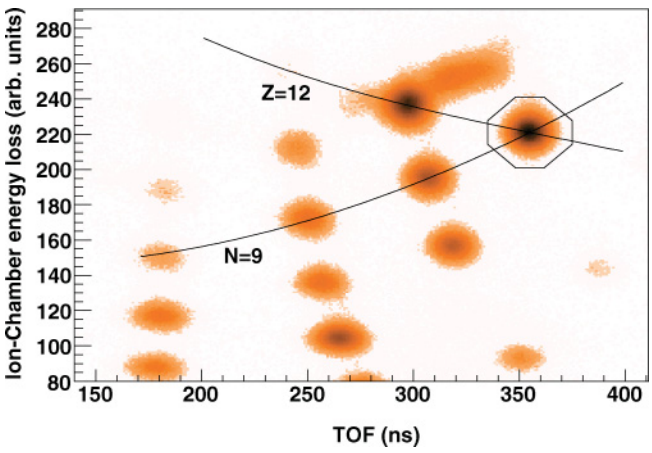

FIG. 2. (Color online) Particle identification of reaction residues in coincidence with incoming ^{22}Mg secondary beam particles. The identification was achieved using the S800 focal-plane detectors [22] as described in the text. The gate used as identification of the $N = 9$, $Z = 12$ ^{21}Mg reaction residue is shown.

In the configuration used for the present measurement, SeGA consists of a forward ring at 37° and a ring at 90° with respect to the beam axis composed of seven and nine detectors, respectively. This forward-focused geometry is optimized for in-beam γ-ray spectroscopy with fast beams as it takes advantage of the Lorentz boost of the γ-ray distribution emitted from fast-moving nuclei. The segmentation of SeGA is used to event-by-event Doppler reconstruct the γ rays emitted by the knockout residues in flight. A full-width-at-half-maximum energy resolution of 25 keV at 900 keV was achieved. The SeGA configuration used here yielded a photopeak efficiency of 2.5% at 900 keV for a stationary source and a corresponding in-beam efficiency of 3% with the Lorentz boost of the γ-ray distribution taken into account.

III. RESULTS AND DISCUSSION

A. In-beam γ-ray spectroscopy

With complete particle identification in the incoming and all exit channels, the γ rays emitted in the ^{9}Be(^{22}Mg,^{21}Mg)X reaction were selectively measured. The Doppler-corrected γ-ray spectrum is shown in Fig. 3, where five γ-ray transitions are identified and labeled with their energy. The region below the strong 888-keV transition in the spectrum shows only the corresponding Compton continuum and no evidence for additional photopeaks at lower energy was found.

It is evident from comparison to Fig. 1(c), that the energies of all five γ-ray peaks are consistent with the

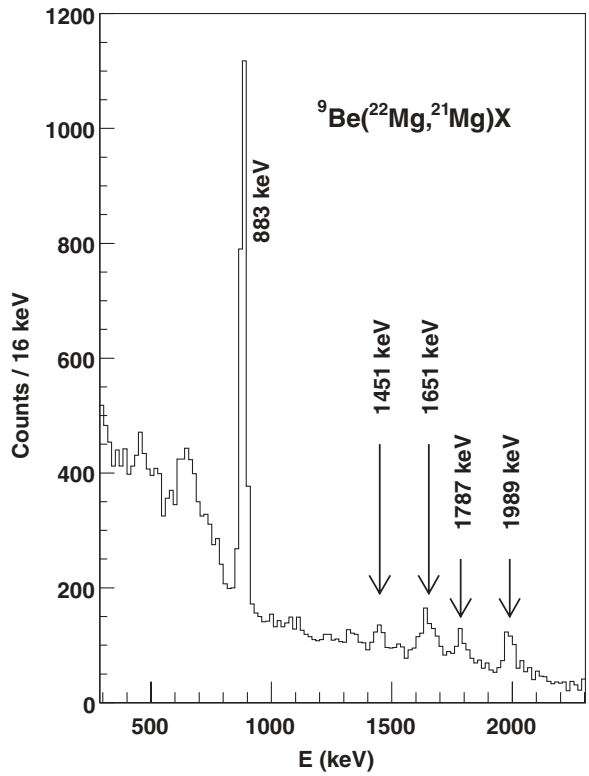

FIG. 3. Doppler-corrected energy spectrum for γ rays emitted by ^{21}Mg in the one-neutron knockout from ^{22}Mg.

previously proposed level scheme. The most intense transition corresponds to the decay of the 1084-keV state to the 201-keV $1/2^+$ state, whereas the other, weaker transitions are attributed to the decays of two higher-lying states to the $5/2^+$ ground state and to the $1/2^+$ first excited state. With these assignments of γ-ray transitions, the energies of the bound excited states are measured with better precision than previously achieved in particle spectroscopy [1651(4) keV and 1989(3) keV, respectively].

The energy of the $1/2^+$ first excited state is found from energy differences of γ-ray transitions from the 1651(4) and 1989(3)-keV states to the ground state and the first excited states, respectively. This yields the most precise individual measurement of this level energy so far with an energy determined to be 201(4) keV. The γ decay of the $1/2^+$ state could not possibly be observed in an in-beam experiment, as the low decay energy and the $E2$ character of the transition to the $5/2^+$ ground state make the state isomeric. With the energy difference between the two mirror states taken into account, the isomeric nature of the ^{21}Mg $1/2^+$ state is predicted from the corresponding mirror-state half-life of 6.1(6) ns [8]. From this—assuming the transition matrix elements to be identical for the two mirror transitions and knowing the $E2$ character of the transition—the half-life of the $1/2^+$ state in ^{21}Mg is estimated to be approximately 32 ns. This leaves the state to decay on average 5.2 m downstream of the reaction target, far beyond the reach of SeGA. The previously adopted level energy [8] is the result of a weighted average of several existing measurements based on particle spectroscopy.

The question arises whether the significant energy shift observed for the $1/2^+$ state can be attributed to the Thomas-Ehrman effect [25,26]. The occupancies of the $s_{1/2}$ orbital (calculated with the shell model using the USDB effective interaction) for the $5/2^+$, $1/2^+$, and $3/2^+$ states are all similar, 0.50, 0.37, and 0.35, respectively. In addition, the average $s_{1/2}$ orbital separation energies are all about 7.0 MeV. Thus, we do not expect a large Thomas-Ehrman shift. Charge-dependent two-body interactions contributing to energy shifts in mirror nuclei were considered in Ref. [27]. In Table 5 of [27] the b coefficients for the isobaric mass multiplet equation for the $5/2^+$ and $1/2^+$ states are predicted to be 4.402 and 4.403 MeV, respectively, and we have calculated the value for $3/2^+$ to be 4.386 MeV (for isospin $T = 3/2$ the b coefficient is the binding energy difference divided by three). These can be compared to the experimental values of 4.435(5), 4.408(5), and 4.408(14) MeV, respectively. The error for the $5/2^+$ ground-state coefficient is from the experimental uncertainty of 0.016 MeV in the ^{21}Mg ground-state binding energy. The agreement is reasonable compared to the average rms obtained for b coefficients in this mass region of 27 keV from Table II of Ref. [27]. In terms of the excited state energy shifts, the experimental results for $1/2^+$ and $3/2^+$ are $-0.080(4)$ and $-0.080(13)$ MeV compared to the calculated values of 0.002 and -0.052 MeV, respectively.

The measurement of the first-excited-state energy allows for an identification of the energy of the second excited state [1084(4) keV], again found to be consistent with the previous measurements but superior in precision. The γ-ray energies (E_γ) measured as described above, as well as the deduced level energies (E_x), are summarized in Table I.

TABLE I. Given are excitation energies E_x, spin and parity assignments J_i^π, the measured γ-ray transition energies E_γ, the final state populated in the decay J_f^π, and the branching ratios for the γ decays to the $5/2^+$ ground state and the $1/2^+$ first excited state. No photopeak indicating a γ-ray transition is seen at 1084 keV and a 95% one-sided confidence limit is given (marked with an asterisk).

E_x (keV)	J_i^π	E_γ (keV)	J_f^π	B.R. (%)
1084(4)	$1/2^-$	883.3(8)	$1/2^+$	>95.4*
		1084	$5/2^+$	<4.6*
1651(4)	3/2	1451(4)	$1/2^+$	18(7)
		1651(4)	$5/2^+$	82(7)
1989(3)	$3/2^-$	1787(4)	$1/2^+$	40(8)
		1989(3)	$5/2^+$	60(8)

This first determination of the decay pattern of bound excited states in ^{21}Mg can be used to support or reject previously proposed spin and parity assignments from the selection rules inherent to the multipolarity of γ-ray radiation. Because the spins and parities are known for the ground state and the first excited state, the γ-decay branching ratios to those two states can be used to constrain the properties of the feeding states. The experimental branching ratios are summarized in Table I and discussed below.

For the 1084-keV state, only a decay to the $1/2^+$ state is seen, which—together with the previous determination of its $\ell = 1$ orbital angular momentum [4]—favors an assignment of $J^\pi = 1/2^-$ over $J^\pi = 3/2^-$, consistent with the mirror nucleus and shell-model predictions [Figs. 1(a) and 1(b)]. This conclusion is further strengthened by the good correspondence between the observed and calculated cross sections, as will be described in Sec. III B.

The decay pattern of the 1989-keV state is quite different as this state with $\ell = 1$ assignment [4] decays to the $5/2^+$ ground state as well as to the $1/2^+$ first excited state. The state is thus highly unlikely to have spin and parity $J^\pi = 1/2^-$ because the suppression of $M2$, $E3$ multipolarity would strongly hinder the γ decay to the ground state. We therefore assign spin and parity $J^\pi = 3/2^-$ to the state at 1989 keV.

Similarly for the 1651-keV state—with previously proposed assignment of $J^\pi = 1/2^-, 3/2^-$ [8]—the observed decay to the $5/2^+$ ground state excludes a spin-parity assignment of $J^\pi = 1/2^-$ and the assignment of $J^\pi = 3/2^-$ is strongly favored. From the three-neutron transfer experiment, $\ell = 1$ orbital angular momentum was assigned based on the assumption that only a single state at this energy was populated in the ^{24}Mg(^{3}He,^{6}He)^{21}Mg transfer reaction [4]. According to the shell-model calculation and the data from the mirror nucleus, however, an additional state, possibly with spin and parity $9/2^+$, may be present at this excitation energy. The energy difference might be too small to be resolved in the reaction studies that rely on particle detection. This possibility was not considered in the discussion of the previous transfer experiment, and positive parity should not be excluded for this state. In the case of positive parity, $1/2^+$, $3/2^+$, and $5/2^+$ states would be possible with $M1$ or $E2$ transitions to the ground state

TABLE II. Measured and calculated cross sections. Given are the experimental partial cross sections σ_{exp}, calculated single-particle cross sections σ_{sp} from eikonal reaction theory, spectroscopic factors C^2S from WBP shell-model calculations, resulting total theoretical cross sections σ_{th}, and the reduction of the experimental single-particle strength relative to theory $R_s = \sigma_{exp}/\sigma_{th}$. See Sec. III B for discussion of theoretical uncertainties.

E_x (keV)	$n\ell j$	σ_{exp} (mb)	C^2S	σ_{sp} (mb)	σ_{th} (mb)	R_S	S'_n (MeV)
0	$1d_{5/2}$	10.4(18)	1.38	15.1	22.8	0.35(6)	19.4
201	$2s_{1/2}$		0.41	14.9	6.6		19.6
1084	$1p_{1/2}$	5.5(6)	1.70	11.8	21.0	0.26(3)	20.5
1651	$1d_{3/2}$	2.2(6)	0.10	13.9	1.6	1.4(4)	21.0
1989	$1p_{3/2}$	1.7(3)	0.28	12.6	3.6	0.45(8)	21.4
Inclusive		19.7(16)			55.6	0.35(3)	

and the first excited $1/2^+$ state. Of these, $J^\pi = 3/2^+$ is the only possibility consistent with the mirror nucleus and is therefore favored. Experimentally, however, the only J^π assignment that could be excluded was $1/2^-$. We note that, in contrast to the previous three-neutron transfer experiment of Ref. [4], the possibility of a complex-structure, collective $9/2^+$ excited state does not affect the experiment presented here, because such a state would be populated only in a higher-order process (e.g., in the knockout from an excited state of the projectile), which is an unlikely two-step process that, to our knowledge, has not been observed in ^{9}Be-induced one-nucleon knockout reactions to date.

B. Cross sections

The inclusive cross section for the knockout reaction ^{9}Be(^{22}Mg,^{21}Mg)X was determined to $\sigma = 19.7(16)$ mb. The observables and uncertainties that enter the cross-section calculation are the number of ^{22}Mg projectiles (relative uncertainty: $\delta = 0.7\%$), the acceptance of the spectrograph for the residual ^{21}Mg nuclei ($\delta = 8\%$), the target thickness ($\delta = 2\%$), and the number of reaction residues ($\delta = 1\%$).

From the γ-ray spectroscopy as described in the preceding section, partial cross sections for the knockout to the three measured excited states are deduced assuming negligible feeding to these states from unobserved, higher-lying states. This assumption is justified, first, because no γ-ray transitions other than the ones already described are seen and, second, because high-energy γ rays (outside the dynamic range of the γ-ray detectors) are very unlikely, because those would correspond to states well above the proton threshold, and thus one would expect strongly competing proton decay branches. The only bound state other than the observed that should be accessible by one-neutron knockout is the 3086(15)-keV state [4]. According to shell-model calculations, however, the knockout to possible states at 3 MeV will proceed with very small spectroscopic factors between 0.00 and 0.04, depending on the structure of the state. This would correspond to a measured cross section of about 0.0–0.2 mb, assuming a reduction factor similar to that observed. This cross section would correspond to about one-tenth of the intensity of the weakest observed γ-ray transitions (Fig. 3) and is thus below the sensitivity limit of the present experiment, independent of the γ-decay energy of the involved states. Furthermore, the best estimate of the systematic uncertainty on the measured partial cross sections introduced by unobserved decays of higher-lying states is therefore 0.1 mb, which is negligible compared to other uncertainties (Table II) and the assumption of negligible feeding is thus justified. The measured partial cross sections to the second, third, and fourth excited states are listed in Table II along with the remaining measured cross section, which has to be attributed to knockout to the ground state and the first excited isomeric state.

The theoretical cross sections for the knockout to the individual final states with quantum numbers J^π are calculated as:

$$\sigma_{th}(E_x, J^\pi) = \left(\frac{A}{A-1}\right)^N C^2S(n\ell j, J^\pi)\sigma_{sp}(n\ell j, S'_n).$$

Here the single-particle cross sections $\sigma_{sp}(n\ell j, S'_n)$ for the removal of a neutron with quantum numbers $n\ell j$ depends on the effective separation energy $S'_n = S_n + E_x$ of the neutron relative to the (excited) final state and is calculated by taking into account the contributions from diffractive breakup as well as stripping; the calculations employ the eikonal reaction theory of Refs. [12–14] with potentials and input parameters related to nuclear sizes chosen as described in Refs. [28,29]. The spectroscopic factors $C^2S(n\ell j, J^\pi)$ describe the structural overlap between the initial- and final-state wave functions—the ^{22}Mg ground state and the final state of ^{21}Mg—and are calculated with the shell-model code NuShell@MSU [9] using the WBP effective interaction [10]. Because the projectile ^{22}Mg has a 0^+ ground state, only one term $(n\ell j)$ contributes to the cross section for each final single-hole state. A center-of-mass correction $[A/(A-1)]^N$ with N being the major oscillator quantum number (see Ref. [14] for more details) has been applied to the shell-model spectroscopic factor. The extracted spectroscopic information is summarized in Table II.

The measured cross sections are significantly lower than the calculated values that rely on the spectroscopic factors from the shell-model calculations. A reduction of experimental spectroscopic strengths to 60–70% of independent-particle model predictions has been established from electron-induced single-proton knockout reactions performed on stable nuclei [30] and is ascribed to a variety of correlation effects missing in the present effective-interaction theories [31,32]. A stronger

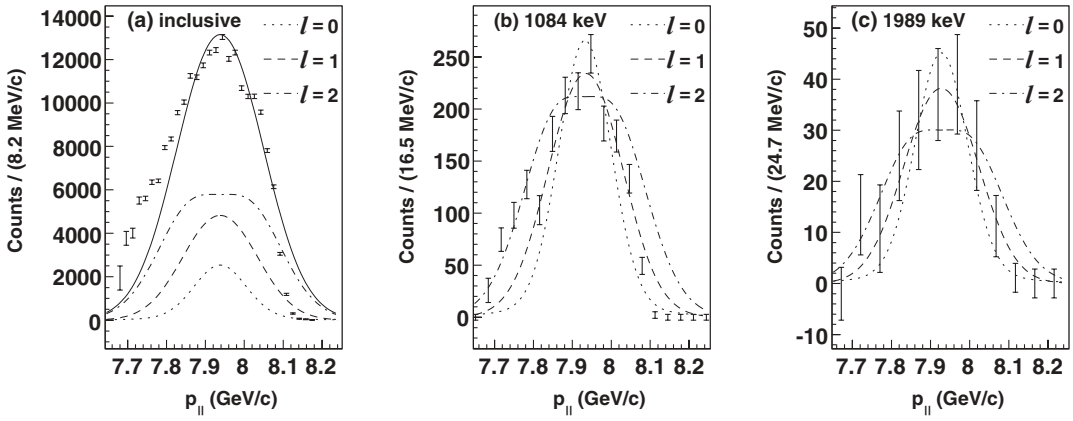

FIG. 4. Background-subtracted, acceptance-corrected momentum distributions for the one-neutron knockout to ^{21}Mg. The inclusive momentum distribution (a) and the momentum distributions for knockout to the 1084- and 1989-keV levels (b) and (c) are shown. Theoretical distributions for orbital angular momenta $\ell = 0$, $\ell = 1$, and $\ell = 2$ are shown as dotted, dashed, and dot-dashed lines, respectively. For the inclusive momentum distribution the individual contributions are added according to the partial cross sections listed in Table II. In all cases, the theoretical distributions are scaled to match the amplitude and centroid of the measured distribution.

reduction down to 24% of the shell-model spectroscopic strength has been found in the removal of strongly bound neutrons from proton-rich nuclei and a dependence of the amount of the reduction on the asymmetry at the Fermi surface has been discussed [28,33]. The reduction factor, $R_S = \sigma_{\rm exp}/\sigma_{\rm th}$, that quantifies this quenching is 0.35(3) for the inclusive cross section of the knockout from ^{22}Mg to ^{21}Mg and is given in Table II also for the removal leading to individual final states of ^{21}Mg. In all cases, the uncertainties are solely experimental. To estimate the theoretical uncertainties, the spectroscopic factors C^2S for the $5/2^+$, $1/2^+$, and $3/2^+$ states, have—using the USDB interaction—been calculated to 1.43, 0.38, and 0.08, respectively, yielding a difference of 0.02–0.05 compared to the WBP calculations. The reduction factors encountered in the present work are generally around 0.35 and thus consistent with the trend, scale, and fluctuations of previous measurements where a strongly bound neutron is removed from an already neutron-deficient nucleus [33]. The only deviation is found for the 1651-keV state; the spectroscopic factor for this state, however, is very small and one might—in addition to the large experimental uncertainty—expect the relative theoretical uncertainty for the shell-model calculation to be large.

C. Momentum distributions

The shape of the parallel-momentum distribution of the residual nucleus depends on the ℓ-value of the knocked-out nucleon and can thus be used to assign orbital angular momentum quantum numbers to specific final states in the projectile-like knockout residue (e.g., see Ref. [14]). The inclusive parallel-momentum distribution is shown in Fig. 4(a), where a correction from the (measured) angular acceptance of the S800 spectrograph as a function of residue momentum has been taken into account. The theoretical momentum distributions have been calculated for knockout of nucleons from s, p, and d single-particle states using the method described in Refs. [16,17]. For the comparison to the inclusive momentum distribution, the calculated shapes have been added according to the measured partial cross sections given in Table II, with the ratio of partial cross sections to the $1d_{5/2}$ and $2s_{1/2}$ states taken from the theoretical calculation. The sum distribution is scaled to match the height and centroid of the measured distribution, where the relative centroid shifts in Figs. 4(a), 4(b), and 4(c) were less than 10 MeV/c. The calculated and measured distributions are consistent but show the same asymmetry in the measured distribution with enhancement at low momenta as has been seen in previous knockout experiments [29,34]. This asymmetry dominates below 7.8 GeV/c, as is apparent from Fig. 4(a). At high momenta (above 8.1 GeV/c), an acceptance cut is observed, for which reason only data with parallel momentum between 7.8 and 8.1 GeV/c were included in the comparison to the theoretical momentum profile (see Fig. 4). This acceptance cut dominated the uncertainty in the calculation of the inclusive cross section (Sec. III B).

The momentum distributions for the knockout to the 1084-keV level and the 1989-keV level have been extracted and are shown in Figs. 4(b) and 4(c). When excluding the low-momentum tail as discussed above and taking into account the high-momentum cutoff, it is seen that the momentum distribution for the 1084-keV level suggests an $\ell = 1$ knockout, confirming the previous assignment of a state from the p shell [4]. The momentum distribution for the 1989-keV state [Fig. 4(c)] is also consistent with the previous $\ell = 1$ assignment by Ref. [4], but the uncertainty in the measured distribution is too large to make a firm assignment based on the present data. For the 1651-keV state the statistics and the background discrimination were not sufficiently good to allow for an extraction of the momentum distribution.

IV. CONCLUSION

In summary, we have performed in-beam γ-ray spectroscopy of ^{21}Mg for the first time, using the ^{9}Be(^{22}Mg,^{21}Mg)X

one-neutron-knockout reaction at 74 MeV/nucleon. Five γ-ray transitions have been identified in ^{21}Mg. The resulting excitation energies are consistent with previous particle spectroscopy data and the precision was improved significantly by the present experiment. The energy of the isomeric first excited state was determined indirectly through γ-ray energy differences. Spin and parity assignments for higher excited states in ^{21}Mg have been constrained through the measurement of the γ-decay patterns. All spin assignments proposed here are consistent with the states observed in the mirror nucleus ^{21}F and with the WBP shell-model calculations; the assignment from experiment alone was not conclusive only for the 1651-keV state. The inclusive cross section for the knockout reaction and the partial cross sections for the population of individual final states were measured and found to agree with shell-model calculations and eikonal reaction theory when taking into account the appropriate reduction factor. This agreement was found for all states when uncertainties were taken into account.

In conclusion, the present experiment confirms the predictions of shell-model calculations for ^{21}Mg through measurement of the low-lying level scheme. With the combined measurement of spins and spectroscopic factors, the agreement lends confidence to shell-model calculations for ^{21}Mg as these are crucial input to calculations of the astrophysical rp-process reaction rates, in particular for the ^{20}Na$(p, \gamma)^{21}$Mg reaction rate.

ACKNOWLEDGMENTS

This work was supported by the National Science Foundation under Grants PHY-0606007 and PHY-0555366 and the United Kingdom Science and Technology Facilities Council (STFC) under Grant EP/D003628.

[1] M. Wiescher, J. Görres, F.-K. Thielemann, and H. Ritter, Astron. Astrophys. **160**, 56 (1986).
[2] A. St. J. Murphy *et al*., Phys. Rev. C **73**, 034320 (2006).
[3] G. Audi, A. H. Wapstra, and C. Thibault, Nucl. Phys. **A729**, 337 (2003).
[4] S. Kubono *et al*., Nucl. Phys. **A537**, 153 (1992).
[5] W. Benenson, E. Kashy, and I. D. Proctor, Phys. Rev. C **8**, 210 (1973).
[6] R. Pardo, in *Proceedings of the 6th International Conference on Atomic Masses and Fundamental Constants* (AMCO-6), edited by J. A. Nolen and W. Benenson (Plenum Press, New York, 1980), p. 25.
[7] G. W. Butler, J. Cerny, S. W. Cosper, and R. L. McGrath, Phys. Rev. **166**, 1096 (1968).
[8] R. B. Firestone, Nucl. Data Sheets **103**, 269 (2004).
[9] NuShell@MSU, B. A. Brown and W. D. M. Rae (2007), MSU-NSCL report, www.nscl.msu.edu/brown/resources/.
[10] E. K. Warburton and B. A. Brown, Phys. Rev. C **46**, 923 (1992).
[11] B. A. Brown and W. A. Richter, Phys. Rev. C **74**, 034315 (2006), www.nscl.msu.edu/brown/resources/.
[12] J. A. Tostevin, Nucl. Phys. **A682**, 320c (2001).
[13] J. A. Tostevin, J. Phys. G **25**, 735 (1999).
[14] P. G. Hansen and J. A. Tostevin, Annu. Rev. Nucl. Part. Sci. **53**, 219 (2003).
[15] A. Gade and T. Glasmacher, Prog. Part. Nucl. Phys. **60**, 161 (2008).
[16] C. A. Bertulani and P. G. Hansen, Phys. Rev. C **70**, 034609 (2004).
[17] C. A. Bertulani and A. Gade, Comput. Phys. Commun. **175**, 372 (2006).
[18] F. Marti, P. Miller, D. Poe, M. Steiner, J. Stetson, and X. Y. Wu, in *CP600, Cyclotrons and Their Applications 2001, Sixteenth International Conference*, edited by F. Marti (American Institute of Physics, 2001), p. 64.
[19] D. J. Morrissey, B. M. Sherrill, M. Steiner, A. Stolz, and I. Wiedenhoever, Nucl. Instrum. Methods B **204**, 90 (2003).
[20] A. Gade *et al*., Phys. Rev. C **76**, 024317 (2007).
[21] D. Bazin, J. A. Caggiano, B. M. Sherrill, J. Yurkon, and A. Zeller, Nucl. Instrum. Methods B **204**, 629 (2003).
[22] J. Yurkon, D. Bazin, W. Benenson, D. J. Morrissey, B. M. Sherrill, D. Swan, and R. Swanson, Nucl. Instrum. Methods A **422**, 291 (1999).
[23] M. Berz, K. Joh, J. A. Nolen, B. M. Sherrill, and A. F. Zeller, Phys. Rev. C **47**, 537 (1993).
[24] W. F. Mueller, J. A. Church, T. Glasmacher, D. Gutknecht, G. Hackman, P. G. Hansen, Z. Hu, K. L. Miller, and P. Quirin, Nucl. Instrum. Methods A **466**, 492 (2001).
[25] J. B. Ehrman, Phys. Rev. **81**, 412 (1951).
[26] R. G. Thomas, Phys. Rev. **88**, 1109 (1952).
[27] W. E. Ormand and B. A. Brown, Nucl. Phys. **A491**, 1 (1989).
[28] A. Gade *et al*., Phys. Rev. Lett. **93**, 042501 (2004).
[29] A. Gade *et al*., Phys. Rev. C **69**, 034311 (2004).
[30] L. Lapikás, Nucl. Phys. **A553**, 297 (1993).
[31] W. H. Dickhoff and C. Barbieri, Prog. Part. Nucl. Phys. **52**, 377 (2004).
[32] V. R. Pandharipande, I. Sick, and P. K. A. deWitt Huberts, Rev. Mod. Phys. **69**, 981 (1997).
[33] A. Gade *et al*., Phys. Rev. C **77**, 044306 (2008).
[34] A. Gade *et al*., Phys. Rev. C **71**, 051301(R) (2005).